This is an *Accepted Manuscript*, which has been through the Royal Society of Chemistry peer review process and has been accepted for publication.

Accepted Manuscripts are published online shortly after acceptance, before technical editing, formatting and proof reading. Using this free service, authors can make their results available to the community, in citable form, before we publish the edited article. We will replace this *Accepted Manuscript* with the edited and formatted *Advance Article* as soon as it is available.

You can find more information about *Accepted Manuscripts* in the **Information for Authors**.

Please note that technical editing may introduce minor changes to the text and/or graphics, which may alter content. The journal's standard **Terms & Conditions** and the **Ethical guidelines** still apply. In no event shall the Royal Society of Chemistry be held responsible for any errors or omissions in this *Accepted Manuscript* or any consequences arising from the use of any information it contains.

Journal Name

ARTICLE

Insertion and isomerisation of internal olefins at alkylaluminium hydride: catalysis with zirconocene dichloride
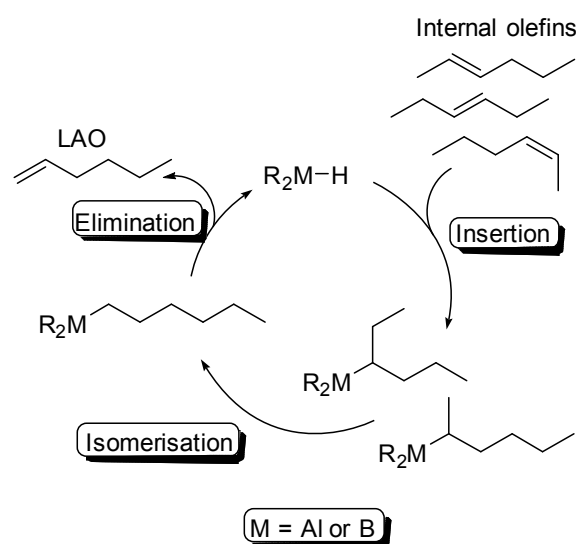
Nandita M. Weliange,[a] David S. McGuinness,*[a] Michael G. Gardiner[a] and Jim Patel[b]

The insertion of internal olefins (hydroalumination) and chain walking isomerisation at di-n-octylaluminium hydride [Al(Oct)$_2$H], promoted by zirconocene dichloride [Cp$_2$ZrCl$_2$] has been studied. The reaction between [Cp$_2$ZrCl$_2$] and [Al(Oct)$_2$H] in non-polar solvents leads to clusters containing bridging hydride ligands between Zr and Al. This system promotes hydroalumination of 1-octene but is largely ineffective for internal octenes (2-, 3-, 4-octene). In tetrahydrofuran the Zr–Al hydride clusters formed are more reactive and catalyse insertion and isomerisation of internal olefins to primary metal–alkyls, although this is accompanied by catalyst deactivation. Elimination and removal of 1-octene from the system post insertion/isomerisation was attempted, but it was found that the presence of the Zr catalyst leads to back-isomerisation to internal octenes, along with futher decomposition with n-octane formation. Some possible pathways of catalyst decomposition, involving reduction of Zr and alkane elimination, have been studied theoretically.

Introduction

Linear α-olefins (LAOs) are an important feedstock of the modern chemical industry.[1] The typical route to produce LAOs involves metal catalysed ethylene oligomerisation,[2-6] and recent research efforts have focussed on the development of catalysts for selective production of co-monomer range olefins (particularly 1-hexene and 1-octene)[7-11]

An attractive potential alternative to ethylene oligomerisation is the conversion of n-alkanes into LAOs. Established industrial processes for alkane dehydrogenation to mono-alkenes do exist, however generally lead to mixtures of predominately internal olefins.[12] The conversion of internal olefins into α-olefins, which is a contrathermodynamic process, is therefore required in order to develop an overall n-alkane to LAO conversion process. For this reason, we have recently[13,14] been investigating the individual steps of the cycle shown in Scheme 1 as a potential method for internal to α-olefin conversion, which involves three steps. The first is insertion of an internal olefin into a metal-hydride bond to yield a sec-alkylmetal compound. In the second step, which is actually a series of elimination and re-insertion steps (chain walking), the sec-alkyl group undergoes isomerisation to form the thermodynamically preferred primary alkyl. The final step involves β-hydride elimination of an α-olefin and, if done under kinetic control (rapid removal of the liberated olefin from the system), may lead to α-olefin selectively.

a. School of Physical Sciences – Chemistry, Private Bag 75, Hobart 7001, Australia.
   Email: david.mcguinness@utas.edu.au
b. CSIRO Energy, 71 Normanby Rd, Clayton North 3169, Australia.
Electronic Supplementary Information (ESI) available: additional supporting NMR spectra and optimised geometries and energies of all stationary points. See DOI: 10.1039/x0xx00000x

**Scheme 1.** Proposed group 13-hydride based cycle for contrathermodynamic isomerisation of olefins.

For alkylboranes, the first two steps are reasonably facile,[15,16] but we were unable to effect elimination and isolation of α-olefins on a preparative scale,[13] despite reports to the contrary.[17,18] On the other hand, we showed that α-olefins can be removed from tri-n-alkylaluminium with very high selectivity (>97%), but in this case insertion and isomerisation of internal olefins was unsuccessful.[14] The reaction of [Al(n-Alk)$_2$H] with internal olefins reaches an equilibrium position (ca. 50% insertion), and isomerisation to the more stable primary alkyl is too slow to drive the reaction to completion. We have therefore started investigating the use of transition metal catalysts to promote the insertion and

isomerisation steps at aluminium hydrides. Metal catalysed hydroalumination of alkenes and alkynes (Scheme 2) has been widely studied[19-21] and can be considered as an insertion into a transition metal hydride (rapid) followed by transalkylation with aluminium, although this is probably an over simplification in many cases. While the majority of catalysed hydroaluminations involve terminal olefins, a number of these catalysts are also capable of olefin isomerisation,[22-24] and some also promote secondary to primary alkyl conversion on their own. The classic example is Schwartz's reagent, [Cp$_2$ZrHCl].[25,26] This complex reacts with internal olefins under mild conditions to yield [Cp$_2$ZrCl(n-alkyl)] complexes. In situ analogues, prepared by reacting [Cp$_2$ZrCl$_2$] with alkylaluminium reagents (normally in near stoichiometric ratios), are effective catalysts for hydroalumination and carboalumination of olefins and alkynes (but again, are normally employed for α-olefin conversions).[27,28] For this reason, we were interested in the reactivity of internal olefins with the [Cp$_2$ZrCl$_2$]/alkylaluminium system, ultimately with catalytic loadings of zirconium, and report here our studies in this regard. Furthermore, the effect such an isomerisation catalyst might have on the selectivity of the elimination step was unknown, and is investigated also.
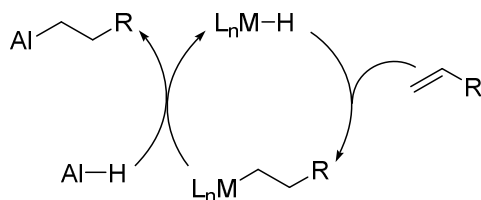

Scheme 2. Metal-catalysed hydroalumination.

The interaction of [Cp$_2$ZrCl$_2$] with [Al^{i}Bu$_3$] and [Al^{i}Bu$_2$H], and the hydroalumination of α-olefins with this system, has been studied in depth by Parfenova, Dzhemilev and Khalilvo (PDK),[27-32] and also Schwartz.[33,34] Bercaw and Brintzinger have further clarified the reactivity of zirconocenes with alkylaluminium hydrides.[35-37] We have drawn on the studies of these groups to aid in understanding of some of the results observed herein.

Results and Discussion

The reactions shown in Scheme 1 have been studied with tri-n-octylaluminium [Al(Oct)$_3$] and di-n-octylaluminium hydride [Al(Oct)$_2$H], and the elimination from/insertion of octenes to these. [Al(Oct)$_2$H] is prepared by thermal elimination (T = 170 °C, vacuum) of 1-octene from [Al(Oct)$_3$], and the reaction may be taken to ca. 80% conversion without decomposition.[14] As such, the aluminium hydride reagent employed in this study has a nominal composition of 70-80% [Al(Oct)$_2$H] and 20-30% [Al(Oct)$_3$]. At this composition, and in non-coordinating solvents (toluene, benzene), the actual speciation of aluminium corresponds to complexes **1**, **2** and **3** as the major species, with **3** the most abundant. If this [Al(Oct)$_2$H] is treated with 1-octene in the absence of a catalyst, insertion proceeds

to yield [Al(Oct)$_3$] with a half-life of approximately 30 minutes at 75 °C. Internal octenes (*cis* and *trans* 2-, 3- and 4-octene) insert only partially, as described in the introduction.[14]
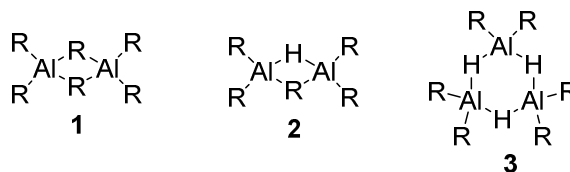

When three equivalents of [Al(Oct)$_2$H] are reacted with [Cp$_2$ZrCl$_2$] in toluene-d_8, the ^{1}H NMR Cp signal at 5.89 ppm is replaced with a signal at 5.65 ppm along with broad Zr-H resonances at -1.06 (1H) and -2.20 ppm (2H). These signals are closely analogous to those observed when [Cp$_2$ZrCl$_2$] is treated with [Al^{i}Bu$_2$H],[33] and the work of Bercaw and Brintzinger suggests the time averaged structure **4** (Reaction 1, R = ^{i}Bu).[35] Integration of the signals observed in our work is likewise indicative of structure **4** (R = n-octyl). This complex is stable in solution for days. Unfortunately all attempts to crystallise it were unsuccessful. The 3:1 Al:Zr stoichiometry is also supported by the observation that less than three equivalents of [Al(Oct)$_2$H] lead to formation of **4** only to the extent dictated by this stoichiometry. Thus, a 1:1 reaction of Al-H with [Cp$_2$ZrCl$_2$] leads to three signals for the [Cp$_2$Zr] moiety, of which 30% is the signal for **4**. With a 2:1 Al-H:Zr ratio, 66% of the [Cp$_2$Zr] signals correspond to **4** (^{1}H NMR spectra at different Al-H:Zr ratios are shown in the Supporting Information, Figure S1). In these sub-stoichiometric cases, the other Cp signals correspond to unreacted [Cp$_2$ZrCl$_2$] and [Cp$_2$ZrCl(Oct)] (**5**). The latter complex gives rise to a cyclopentadienyl signal at 5.79 ppm along with a characteristic multiplet integrating for 2 protons at 1.08 ppm, corresponding to the Zr-CH_2 resonance (60.7 ppm in the ^{13}C NMR spectrum).[25,38] Complex **5** presumably results from chloro/alkyl exchange between [Cp$_2$ZrCl$_2$] and [Al(Oct)$_3$] which is present in our system; others have reported that AlR$_3$ (R = Me, Et) reacts likewise to form mixtures of [Cp$_2$ZrClR] and Cp$_2$ZrCl$_2$.[39,40]

$$\text{Cp}_2\text{ZrCl}_2 \ + \ 3\ \text{AlR}_2\text{H} \longrightarrow \quad (1)$$
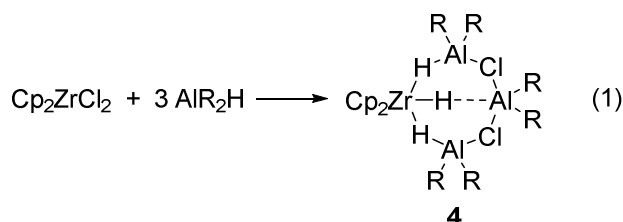
The hydride signals of **4**, which are broad at room temperature, split at low temperature such that the expected[35] coupling (*J* = 7 Hz) between the downfield triplet and upfield doublet is partially resolved at -50 °C (Figure 1). In addition, a number of extra Zr-hydride signals are observed at low temperature (-1.15, -1.92 and -2.38 ppm at -50 °C). These indicate one or a number of additional Zr–hydride complexes are present in addition to **4**, which undergo exchange/equilibrium processes with one another.[‡] The PDK

group observed a signal at -1.94 ppm which was attributed to complex **6** (R = ^{i}Bu), and proposed two equal intensity signals at -0.65 to -1.35 and -2.56 to -2.80 ppm are due to complexes such as **7** and **8**.[28,29,33,41] These complexes were observed in systems where **4** (R = ^{i}Bu) was also observed.
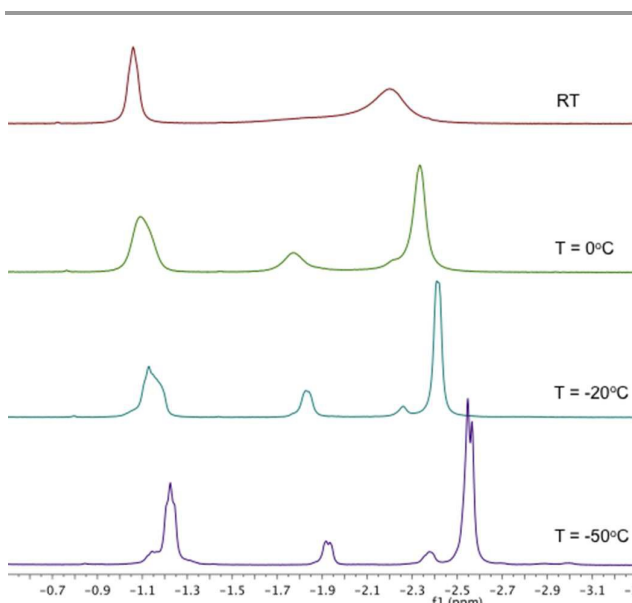
**Figure 1.** VT ^{1}H NMR spectroscopy of the Zr–hydride region of [Cp$_2$ZrCl$_2$] + 3 [Al(Oct)$_2$H] in toluene-d$_8$.

The existence of several species is also evidenced by multiple ^{1}H NMR signals in the Cp region at low temperature (Figure S3). Unfortunately these signals are broad and overlap, so accurate integration of individual species and assessment of possible Zr-H : Cp ratios (which might support formulations such as **6**-**8**) was not possible. The theoretical ^{1}H NMR shielding values for these structures, along with several other possibilities, were calculated and this is discussed in the Supplementary Information. While the calculated ^{1}H NMR shifts for complex **4** are in good agreement with experiment, the agreement between experiment and theory for **6**-**8** is not compelling. Thus, while the *n*-octyl substituted analogues of **6**, **7** and **8** seem possible in our system, we cannot make this assignment with a high level of confidence; these solution structures are suggested only as possibilities based on the spectral similarities with previous work.
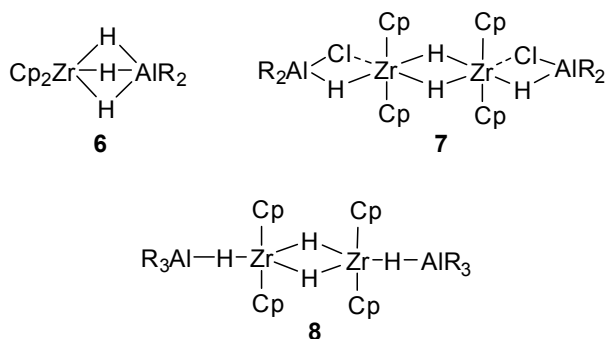
Olefin Insertion

We first investigated the reaction of 1-octene with the [Cp$_2$ZrCl$_2$]/[Al(Oct)$_2$H] system (in toluene), which allows for more straightforward characterisation of the products obtained and also provides for comparisons with subsequent internal olefin addition. When a 1:1 solution of [Cp$_2$ZrCl$_2$] and [Al(Oct)$_2$H] is reacted with one equivalent of 1-octene at room temperature, insertion occurs rapidly and is essentially complete in the time take to acquire a ^{1}H NMR spectrum. Insertion leads to the formation of [Cp$_2$ZrCl(Oct)] (**5**) as the major product (Reaction 2). Along with this, a small amount of [Cp$_2$ZrCl$_2$] (5%) remains along with 7% of complex **4** (by integration of the Cp$_2$Zr signals). Trace olefinic signals for 1-octene are also observed. The residual 1-octene and hydride **4** do not seem to result from incomplete progress of the reaction, as the composition is unchanged after a further hour. Rather, this appears to be the equilibrium position of the reaction. This was confirmed by reacting [Cp$_2$ZrCl$_2$] with [Al(Oct)$_3$], which led to a similar composition of Cp$_2$ZrCl$_2$, **4**, **5** and free 1-octene.
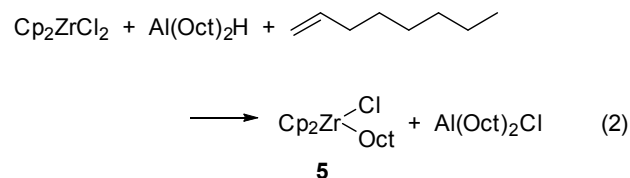
The insertion reaction is significantly slower when an excess of hydride is present in the system (catalytic zirconocene). Thus, a 1:6 solution of [Cp$_2$ZrCl$_2$]:[Al(Oct)$_2$H] treated with half an equivalent of 1-octene (relative to Al-hydride) leads to only 10% insertion of the octene at room temperature after 1 hour (as judged by ^{1}H NMR monitoring). Heating the solution to 60 °C leads to more complete insertion of 1-octene (90% in 45 minutes), but it is clear that excess aluminium hydride severely retards insertion. Similar behaviour has been reported by the PDK group.[27-31] They found that clusters such as **4** are much less active for hydroalumination than less encumbered Zr–hydrides (the most active reagent is thought to be [Cp$_2$ZrHCl]). At high ratios of Al-H/Zr complex **4** is the principal species present, perhaps at the expense of more active Zr–hydrides. This is also analogous to previous studies of catalyzed carboalumination and chain growth, which show that olefin insertion into the M–C bond is hindered by formation of alkyl bridged M/Al dimers, which must break apart prior to olefin coordination and insertion.[42-45]

Unfortunately, this system was found to be even less active for internal olefin insertion. When a thermodynamic mix of octenes (1.5% 1-octene, 10.5% *trans*-4-, 33.4% *cis/trans*-3- and *cis*-4-, 40.5% *trans*-2- and 14.1% *cis*-2-) was reacted, no discernible insertion takes place at room temperature even with an excess of [Cp$_2$ZrCl$_2$] present. Heating the solutions (40–80 °C) leads to variable degrees of olefin conversion but this is accompanied by decomposition. The solutions turn dark purple in colour and numerous signals appear in the

cyclopentadienyl region as well as multiple resonances in the Zr–hydride region. The colour change observed is indicative of reduction of zirconium. A more detailed exploration of this behaviour is described below. These decomposed samples proved intractable. Interestingly, with excess [Al(Oct)$_2$H] present (Al–H/Zr = 6), decomposition of the solution was not observed at elevated temperatures (60 °C, 24 hr). This appears to be because zirconium is locked up in the stable cluster **4**. An undesirable consequence of this stability is very limited octene insertion; ca. 16% over 24 hr.

Given that the formation of stable Zr–Al hydride cluster(s) seems at least partially responsible for low insertion activity,[32] we investigated the effect of THF solvation on the reactivity of the system. The rationale here being that formation of more active mononuclear metal hydrides (with coordinated THF) may occur. As discussed below, this turned out not to be the case, and Zr/Al clusters of some form appear to persist in THF. In the Supplementary Information the reaction free energy of THF coordinating to and breaking apart complex **4** is estimated, and it is found that this reaction is not favourable. Nonetheless, THF does appear to have an effect on the rate of olefin insertion. When a solution of [Cp$_2$ZrCl$_2$] in THF is treated with 1 equivalent of [Al(Oct)$_2$H], the formation of a colourless precipitate is observed. Exchange of the zirconium chloro ligand with alkyl or hydride groups is evidenced by the formation of [Al(Oct)$_2$Cl(THF)] (Al–CH_2 at -0.05 ppm, along with a signal at -0.18 ppm corresponding to [Al(Oct)$_3$(THF)]). The area of the signals for the Cp$_2$Zr moiety relative to the alkylaluminium signals shows that only ca. 30% of the zirconocene remains in solution. The major Zr complex is [Cp$_2$ZrCl$_2$], but this is accompanied by 5 additional Cp$_2$Zr signals (Figure S4). There are also multiple signals in the Zr–hydride region from -0.7 to -4.0 ppm; three signals at room temperature resolving to 7 signals at -50 °C (Figure S5). When [Cp$_2$ZrCl$_2$] is treated with 3 equivalents of [Al(Oct)$_2$H] in THF no visible precipitate is formed to begin with, although over a number of days a small amount of precipitate was observed. The ^{1}H NMR spectrum of the clear solution, while different to a 1:1 mixture, still indicates multiple species. As shown in Figures S6 and S7, there are two main signals for Cp$_2$Zr along with a third smaller one, and multiple Zr–H and Al–H resonances (the latter at 2.9 – 3.8 ppm, not bridging to Zr), dependent again on temperature. It is known from our previous work that homonuclear Al–hydride clusters such as **2** and **3** do not persist in the presence of THF, instead forming [Al(Oct)$_2$H(THF)] with an Al–H resonance at 4.05 ppm.[14] Hence, it seems likely that the Al–H signals at 2.9 – 3.8 ppm result from one or more Al–Zr clusters. The complexity of this system prevented us from identifying the species present, and attempts at crystallisation were unsuccessful. Only the presence of Zr–H and Al–H bonding can be confirmed, most likely resulting from species in Zr–Al clusters.

While it appears Zr/Al clusters are formed in THF, they appear to be reactive with respect to olefin insertion. Thus, despite the limited solubility of a 1:1 mixture of [Cp$_2$ZrCl$_2$] and [Al(Oct)$_2$H] in THF, insertion of 1-octene proceeds rapidly (ca. 15 min to completion) according to Reaction 2. Complex **5** is

formed cleanly (along with a small amount of Cp$_2$ZrCl$_2$), although it is only partially soluble in THF (the ^{1}H NMR spectrum is shown in the Supplementary Information, Figure S8).

Under similar conditions the mixture of internal octenes requires 24 hrs to reach a high degree of insertion (87% at 40 °C). Interestingly, the ^{1}H NMR spectrum is identical to that resulting from 1-octene insertion, with no evidence for the *sec*-alkyl groups expected from insertion of internal octenes. This shows that isomerisation to the terminal position has occurred (Scheme 3). This was confirmed by quenching the solution with D$_2$O, which leads only to 1-d$_1$-octane (^{13}C NMR analysis, Figure S9). Hence, in THF the [Cp$_2$ZrCl$_2$]/[Al(Oct)$_2$H] system appears to lead to an in situ analogue of Schwartz's reagent, Cp$_2$ZrHCl, with similar reactivity.
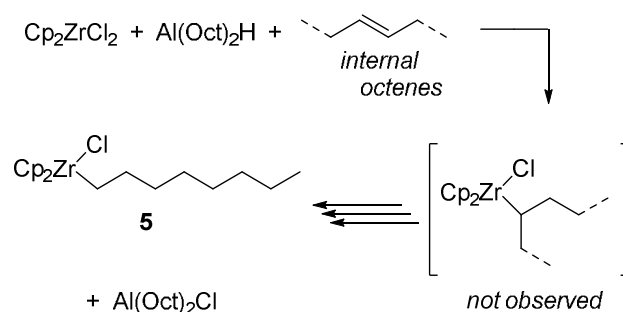
Scheme 3. Insertion and isomerisation of internal octenes.

Encouraged by this result, we attempted internal olefin insertion/isomerisation with excess [Al(Oct)$_2$H]. As is the case in toluene, the reaction is inhibited by excess Al–hydride, but in this case reaches higher conversions. A mixture of [Cp$_2$ZrCl$_2$], [Al(Oct)$_2$H] and internal octenes (1:4:4, 25 mol% Zr) leads to 74% insertion of the olefins after 48 hr at 40 °C. Continuing the reaction for a further 48 hr did not improve the extent of insertion, and it is clear that decomposition or further reactions of the zirconium reagent occur. The solution changes colour to dark purple and, along with the formation of **5**, numerous unidentified additional cyclopentadienyl signals are observed in the ^{1}H NMR spectrum (Figure S10). Additionally, the formation of *n*-octane appears to be associated with this reaction, and is detected in variable amounts by GC-MS analysis. The principal aluminium species present after insertion is [Al(Oct)$_3$(THF)], along with a smaller amount of [Al(Oct)$_2$Cl(THF)] due to halide exchange with Zr (Figure S10). Once again, there is no evidence for *sec*-octyl–metal species in the NMR spectra, and only 1-d$_1$-octane is formed through quenching with D$_2$O. Hence, all octene which has undergone insertion has isomerised to terminal product. It is concluded that the Zr species formed in situ is, at least initially, effective as a *catalyst* for insertion/isomerisation (Reaction 3), but catalyst deactivation occurs along with olefin insertion.

$$Al(Oct)_2H + \quad \xrightarrow[\text{THF}]{\text{Zr cat}} \quad Al(Oct)_3(THF) \quad (3)$$
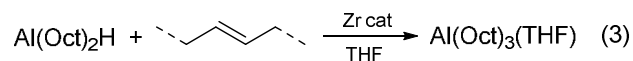
Olefin Elimination

We also investigated olefin elimination in the presence of the Zr catalyst. Selective formation of α-olefin relies on the slow rate of isomerisation at aluminium, coupled with the rapid removal of olefin from the system. The latter requirement is illustrated by the fact that partial isomerisation to internal olefins is observed if product removal is inefficient.[14] With the Zr catalyst in the system, whose role is isomerisation in the first steps, the selective removal of α-olefin may be affected. Indeed, this is the case at the high Zr loadings required to promote insertion. As illustrated in Table 1 (entry 2), when elimination of octene from [Al(Oct)$_3$]/[Al(Oct)$_2$Cl] is carried out in the presence of Zr (90 °C, vacuum, Al/Zr = 3.1), the mixture of octenes collected is substantially isomerised to internal octenes. For comparison, elimination from [Al(Oct)$_3$] without Zr present yields up to 98% 1-octene (entry 3).[14] The major internal octene isomers formed are *cis*- and *trans*-2-octene, in approximately equal amounts. These two isomers are the first products of chain walking from the primary position. Increased loadings of [Cp$_2$ZrCl$_2$] lead to more extensive isomerisation (less 1-octene) and higher percentages of deeper internal olefins (3- and 4-octenes). The selectivity of elimination is not improved by conducting it at higher temperatures. In all cases, elimination causes the reaction mixture to turn deep red in colour, and the formation of *n*-octane is again observed in varying amounts (up to ca. 1 equivalent relative to octene, Table 1, entry 2).

Table 1. Octene elimination from [Al(Oct)$_3$]/[Al(Oct)$_2$Cl] in the presence of zirconocene catalyst [a]

Entry	1-octene	Trans-4	Cis-2	Trans-2	Other[b]
1. Reactant composition[c]	1.5	10.5	14.1	40.5	33.4
2. Eliminated composition[d]	37.8	3.3	24.4	20.0	14.4
3. [Al(Oct)$_3$][e]	97.7	------------------------ 2.3 ------------------------			

[a] Conditions: Al/Zr = 3.1, 90 °C, vacuum. [b] *cis*- and *trans*-3 and *cis*-4-octene. [c] Composition of internal octene mixture prior to insertion and isomerisation. [d] 1.3 equivalents of *n*-octane (relative to octenes) also collected. [e] Elimination from [Al(Oct)$_3$] in the absence of Zr catalyst (170 °C), from reference[14].

As decomposition of the Zr reagent seems to be prevalent during insertion and elimination, some comment on the possible decomposition pathways is appropriate. In the presence of excess Al–hydride, Zr appears to be quite stable, seemingly due to the formation of stable hydride bridged clusters such as **4**. On the other hand, once insertion has occurred and M–hydride has been replaced by M–octyl, the decomposition reaction is observed (either during prolonged insertion experiments, during olefin elimination, or both). This suggests that decomposition occurs from a Zr–octyl species. The decomposition of zirconocene alkyl-hydrides or dialkyls, leading to alkane formation and reduced zirconocene species, is quite well known. For example, dialkyl zirconocenes are known to be a source of "Cp$_2$Zr(II)", which may be trapped by addition of other ligands (Scheme 4a).[46–50] Reductive elimination of alkanes from [Cp$_2$ZrHR] is also observed

(Scheme 4b), again leading to Zr(II) in the first instance.[51,52] A number of groups have reported alkane formation from Zr/Al alkyl/hydride clusters, such as complex **8** (R = Me[41], Et[29]) or analogues of **4**.[35] While we have not observed [Cp$_2$ZrH(Oct)] or [Cp$_2$Zr(Oct)$_2$] in our system, the formation of transient small amounts of these or related species seems quite possible, and may be responsible for the decomposition observed.

The development of strong colour changes accompanying decomposition is also common,[35,53-55] as we have observed in this study (red in toluene, purple in thf). Deep red or crimson coloration appears to be characteristic of Zr(III) formation in these reactions.[48,51] Bercaw has characterised a variety of paramagnetic Zr(III) complexes originating from reduction of constrained geometry zirconocenes.[37] Perhaps more relevant to the current work however are early reports from Schwartz that [Cp$_2$Zr(II)(PR$_3$)$_2$] complexes can form diamagnetic Zr(III) dimers such as **9** with evolution of hydrogen (Reaction 4), in which the cyclopentadienyl ligand is non-innocent in the transformation.[51,56] Despite the complexity of the ^{1}H NMR spectra observed after decomposition (Figure S11), the Cp*H* signals remain sharp and we have not seen any evidence for paramagnetism, thus it appears likely that all species formed are diamagnetic. Schwartz reported ^{1}H NMR signals for the η^5, η^1-cyclopentadienyl ligands in **9** between 6.05–3.97 ppm. While undoubtedly more complex in our reactions, the observation of signals between ca. 6.5–3.5 ppm (in toluene, Figure S11) might suggest multiple species containing this same binding mode of cyclopentadienyl. Certainly it is difficult to envisage the cyclopentadienyl ligand in a normal η^5-binding mode leading to signals over this broad range.

(a)

(b)
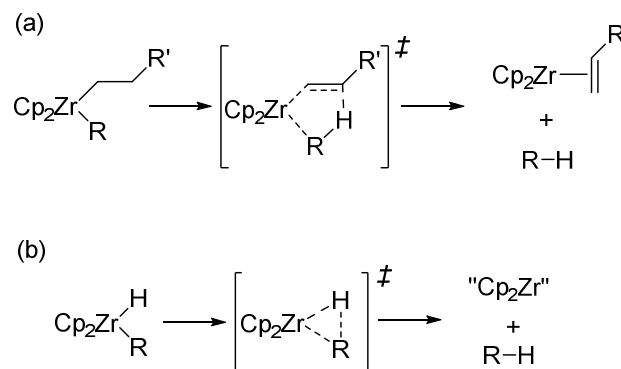
Scheme 4. Alkane elimination routes from Zr(IV) complexes.

$$2\ Cp_2Zr\begin{matrix}PR_3\\PR_3\end{matrix} \longrightarrow \mathbf{9} + H_2 \quad (4)$$
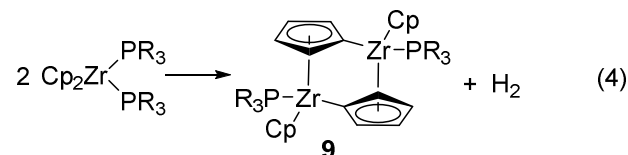
The reduction of zirconium(IV) alkyls according to Scheme 4, followed by pathways to Zr(III) formation, has been probed theoretically (employing a propyl group as a model for the *n*-alkyl chain, see Theoretical Methods section for details). The calculated free energy profiles corresponding to pathways (a)
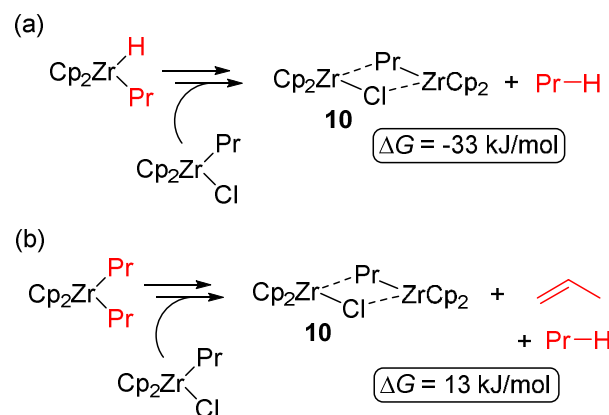
and (b) in Scheme 4 are shown in Figure 2 (free energy estimates have been calculated at 298 K, and hence may be somewhat different under experimental conditions of elevated temperature). Both routes have accessible activation barriers, with the β-hydride transfer barrier (blue trace) a little lower and leading to what is best described as a Zr(IV) metallacyclopropane complex (we could not find a local minimum corresponding to the π-bound propene extreme of bonding). Removal of propene from this species to give [Cp$_2$Zr] and propene is highly endergonic (ΔG = 134 kJ·mol^{-1}), but as discussed below, there are a number of further reactions of the [Cp$_2$Zr] fragment which could overcome this. Likewise, the reductive elimination of propane from [Cp$_2$ZrHPr] is calculated to be unfavourable (ΔG_{react} = 88 kJ·mol^{-1}, red trace in Figure 2). Simple dimerisation reactions of the [Cp$_2$Zr(II)] fragment with Zr(IV) species were found to be downhill, with the most favourable reaction being that with [Cp$_2$ZrPrCl] (a model for the experimentally observed complex **5**). This leads to a closed shell singlet (Zr(III)···Zr(III)) with bridging propyl and chloro ligands (complex **10**, the triplet and antiferromagnetically coupled species (open shell singlet) were also examined and are predicted to be higher in energy, see the supporting information for a full discussion). The stabilisation afforded by dimer formation is sufficient to make reductive elimination favourable, for instance the overall free energy of Scheme 5(a) is ΔG_{react} = -33 kJ·mol^{-1}. A similar dimerisation of the metallacyclopropane complex in Figure 2, with release of propene, is calculated to be moderately endergonic (Scheme 5(b), ΔG_{react} = 13 kJ·mol^{-1}). The formation of such diamagnetic Zr(III) dimers may be one possible route of decomposition.
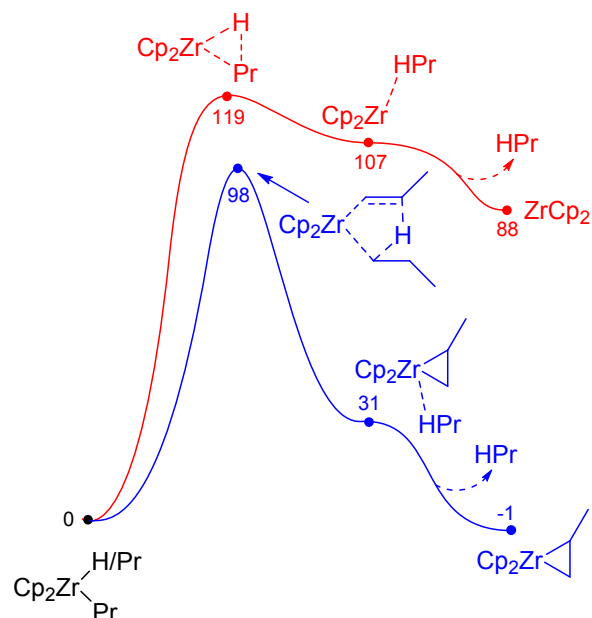
The formation of η^5, η^1-cyclopentadienyl complexes is shown in Figure 3 and appears to correspond closely to that proposed by Schwartz,[56] with some additional subtleties which only become apparent from theoretical studies. The reaction starts with dimerisation of two [Cp$_2$Zr(II)] fragments and appears to involve a number of spin state crossings (singlet to triplet and vice versa) along the path. As is evident in Figure 3, and discussed in the Supplementary Information, the relative spin state energies of several complexes are quite close, so there is some uncertainty in the ground states of these. The free energy surface shown in Figure 3 reflects that calculated with the M06 density functional. The effect of different functionals, and the applicability of DFT for such problems, is discussed in the Supplementary Information.

Oxidative addition of the first cyclopentadienyl C–H bond can occur in the singlet or triplet state, with the latter providing the easiest pathway (**11** → **12** via **TS11-12**). Oxidative addition of the second C–H bond (**12** → **13**) was only located in the singlet spin state, and attempts to optimise the dihydride **13** as a triplet led back to complex **12** in all instances. The binuclear Zr(IV)-Zr(IV) dihydride **13** is the most stable species along the free energy surface. Reductive elimination of hydrogen from singlet binuclear complexes was found not to be favourable, with the easiest route to a dihydrogen complex being a spin state crossing from complex **14** to triplet **15**, where the transition from a dihydride to a dihydrogen complex corresponds to the minimum energy crossing point (MECP).[57] From **15**, the barrier to loss of dihydrogen is very low, leading to the η^5, η^1-cyclopentadienyl dimer **17**, which is calculated to be most stable as a closed shell singlet.

Figure 2. Relative free energies (M06/BS2//M06/BS1, kJ·mol^{-1}, 298 K) for species involved in the reductive elimination of propane from [Cp$_2$ZrPrH] (red) and [Cp$_2$ZrPr$_2$] (blue).

Scheme 5. Calculated energetics of alkane elimination and dimer formation.

The reaction surfaces shown in Figures 2 and 3 are probably an over simplification of the real range of reaction possibilities, particularly given the complexity of the ^{1}H NMR spectrum after decomposition. However they do illustrate that alkane elimination from zirconium(IV) alkyls may be facile, and followed by activation of the cyclopentadienyl ligand, can lead to diamagnetic Zr(IV) and Zr(III) binuclear complexes featuring η^5, η^1-Cp ligation. The presence of alkylaluminium reagents may of course increase the complexity through formation of Zr/Al clusters, and Schwartz[56] has also suggested that
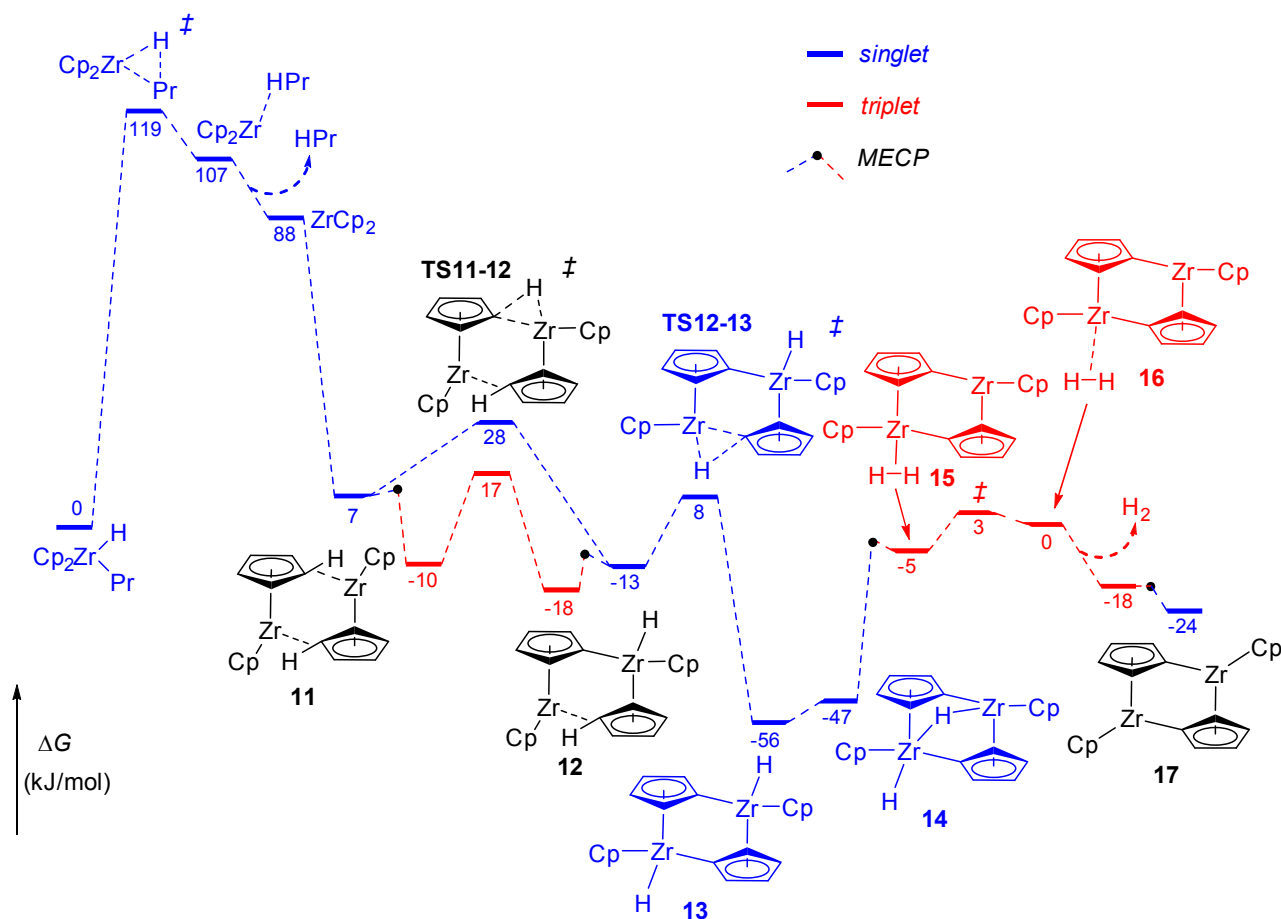
Journal Name

ARTICLE

Figure 3. Relative free energies (M06/BS2//M06/BS1, kJ·mol⁻¹, 298 K) for the reaction [Cp₂ZrPrH] → ½ [CpZr(μ-η¹,η⁵-C₅H₄)]₂ (**17**) + ½ H₂. Energies shown are per mole of Zr (per ½ mole of dimers). Stationary points shown in blue are in the singlet spin state, structures in red triplets, and those in black are calculated in both spin states. The approximate MECP energy levels indicated are derived from M06/BS1 electronic energies.

complexes such as **13** may exist as nonuniform polymers, which we have not considered at this stage. There are also a number of other reduction mechanism possibilities. Bercaw has suggested reduction from homobinuclear Zr(IV) complexes,[37] while Negishi has observed reduction from heterobinuclear (Zr–Al) complexes.[58] Further studies of reduction mechanisms from alkylzirconium(IV) cyclopentadienyl complexes are in progress.

Summary and Conclusion

Herein we have studied the use of zirconocene dichloride to promote insertion of internal olefins (hydroalumination) and

chain walking isomerisation at [Al(Oct)₂H]. The reaction between [Cp₂ZrCl₂] and [Al(Oct)₂H] in non-polar solvent leads preferentially to clusters such as **4**,[35] with bridging hydride ligands, plus a number of other unidentified clusters in equilibrium. In toluene the precatalyst [Cp₂ZrCl₂] promotes hydroalumination of 1-octene, but is largely ineffective for internal octenes. One reason seems to be that the cluster **4** is relatively inert towards insertion,[28] hence its formation, which is favoured at high Al/Zr ratios, limits the use of the Zr reagent in catalytic amounts.

Somewhat more success was achieved in tetrahydrofuran. While it seems Zr/Al hydride clusters are still formed to an extent, it was possible to catalyze the insertion and

isomerisation of internal olefins to primary alkyls (albeit with very high catalyst loadings, ca. 25% Zr). However, this transformation is accompanied by catalyst decomposition/deactivation and alkane formation. Furthermore, the presence of the isomerisation catalyst interferes with the final step of the cycle, leading to back-isomerisation during olefin elimination (whereas this step is highly α-selective in the absence of Zr[14]). The elimination step is also accompanied by further catalyst decomposition. Preliminary observations and theoretical studies suggest that decomposition occurs via reduction of Zr and alkane elimination. From here, binuclear Zr(III) and Zr(IV) complexes may form. We are currently studying the decomposition pathways of Zr(IV)–alkyls in more detail, and investigating alternate catalysts which may be more compatible with the cycle shown in Scheme 1.

Experimental and Theoretical Methods

General

All manipulations were performed under an argon atmosphere using standard Schlenk techniques or carried out in a glovebox. Solvents were purified by passage through an Innovative Technologies solvent purification system and, where appropriate, were stored over a sodium mirror. 1-Octene was dried by distillation over sodium and stored over a sodium mirror. [Al(Oct)$_3$] and [Al(Oct)$_2$H] (70-80% hydride, 20-30% [Al(Oct)$_3$], quantified by ^{1}H NMR) were prepared as described previously.[14] Elimination of octene from [Al(Oct)$_3$] in the presence of Zr catalyst was carried out according to the procedure detailed previously,[14] but at lower temperature (refer to Table 1). NMR measurements were recorded on a Bruker Avance III HD NMR spectrometer with a 5 mm BBFO probe operating at 400 MHz (^{1}H) or 100 MHz (^{13}C). GC–MS analysis was carried out on a Varian 3800 GC coupled to a Varian 1200 triple quadrupole mass spectrometer in single quadrupole mode.

Octylaluminium NMR assignments. In solution with both Al–octyl and Zr–Octyl species present, the NMR assignments for [Al(Oct)$_3$(thf)], [Al(Oct)$_2$Cl(thf)] (in thf-d$_8$) and [Al(Oct)$_{3-n}$Cl$_n$]$_2$ (n ≈ 1, in toluene or benzene) were identified by comparison to independent samples. In the last case, the approximate composition expected from complete insertion of 1-octene into a 1:1 mixture of [Cp$_2$ZrCl$_2$]:[Al(Oct)$_2$H] was prepared by reacting [Al(Oct)$_3$] with [AlCl$_3$] at a 3:1 ratio in toluene. The most characteristic ^{1}H NMR signal distinguishing the different species is the Al-CH_2 multiplet, which resonates at: [Al(Oct)$_3$]$_2$, 0.56 ppm (toluene-d$_8$); [Al(Oct)$_{3-n}$Cl$_n$]$_2$ (n ≈ 1), 0.44 ppm (toluene-d$_8$); [Al(Oct)$_3$(thf)], -0.16 ppm (thf-d$_8$); [Al(Oct)$_2$Cl(thf)], -0.05 ppm (thf-d$_8$). The ^{13}C NMR assignments for [Cp$_2$ZrCl(Oct)] (**5**), [Al(Oct)$_2$Cl(thf)] and [Al(Oct)$_3$(thf)] in a mixed system (after 1-octene has inserted) are shown in Figure S12 (full assignments for **5** are detailed below).

Preparation and characterisation of [Cp$_2$ZrH(μ-H)$_2$Al$_3$(Oct)$_6$(μ-Cl)$_2$] (4). Inside a glove box, Cp$_2$ZrCl$_2$ (15.3 mg, 52 μmol) was added to an NMR tube and dissolved in ca. 0.40 mL of toluene-

d$_8$. To this solution [Al(Oct)$_2$H] (75 μL, 150 μmol hydride, 66 μmol [Al(Oct)$_3$]) was added. The solution became pink in colour. ^{1}H NMR (toluene-d$_8$): δ 5.69 (s, 10H, CpH); 1.64 (m, 12H, CH_2); 1.25-1.55 (br, m, 60H, CH_2); 0.92 (t, J = 7 Hz, 18H, CH_3); 0.38 (t, J = 8 Hz, 12H, AlCH_2); -0.98 (br s → t, J = 7 Hz, 1H, Zr–H); -2.11 (br s → d, J = 7 Hz, 2H, Zr–H). ^{13}C NMR (toluene-d$_8$): δ 104.7 (Cp); 36.2, 32.5, 30.1, 30.0, 26.0, 23.2 (CH_2); 14.4 (CH_3); 10.5 (br, Al–CH_2). The ^{1}H and ^{13}C NMR spectra are shown in Figures S13 and S14

Preparation and characterisation of [Cp$_2$ZrCl(Oct)] (5). This complex can be prepared cleanly in-situ from a 1:1:1 mixture [Cp$_2$ZrCl$_2$]:[Al(Oct)$_2$H]:1-octene in toluene or thf. Thus, [Cp$_2$ZrCl$_2$] (15.4 mg, 53 μmol) was taken up in 0.5 mL of toluene-d$_8$ in an NMR tube and [Al(Oct)$_2$H] (25 μL, 50 μmol hydride, 22 μmol [Al(Oct)$_3$]) and 1-octene (8.0 μL, 51 μmol) added. ^{1}H NMR (toluene-d$_8$): δ 5.79 (s, 10H, CpH); 1.2-1.7 (m, br, CH_2, overlapping with Al-octyl signals); 1.08 (m, 2H, ZrCH_2); 0.90 (m, CH_3 overlapping with Al-octyl signals). ^{13}C NMR (toluene-d$_8$): δ 113.0 (Cp); 60.7 (ZrCH_2); 36.4 (γ-CH_2); 34.6 (β-CH_2), 32.6, 29.8, 23.2 (CH_2); the CH_2 signal at 30.0 ppm and the CH_3 at 14.4 ppm are masked by the corresponding Al-octyl signals. Complex **5**, displaying the same spectral properties, can be independently prepared by reacting Cp$_2$ZrHCl with 1-octene, as reported by Schwartz.[25] The ^{13}C NMR spectrum in toluene-d$_8$ is shown in Figures S15-S17. In thf, several of the CH_2 signals in the ^{1}H NMR spectrum are better resolved from the signals due to Al-octyl species, such that the β- and γ-methylene signals can be assigned in addition to the α-resonance; ^{1}H NMR (thf-d$_8$): d 6.21 (s, 10H, CpH); 1.54 (m, 2H, β-CH_2); 1.25-1.50 (br, CH_2 Zr-octyl and Al-octyl); 1.16 (m, 2H, γ-CH_2); 0.99 (m, 2H, ZrCH_2); 0.88 (m, CH_3 Zr-octyl and Al-octyl). Assignment of the α, β and γ ^{1}H and ^{13}C NMR signals was based on COSY correlations between the α and β hydrogens and between β with both α and γ, and with HSQC correlations for the ^{13}C assignments.

Olefin insertion. A representative example corresponds to attempted insertion of a mixture of octene isomers into [Al(Oct)$_2$H] with 25 mol% [Cp$_2$ZrCl$_2$] as catalyst: Inside the glove box, [Cp$_2$ZrCl$_2$] (18.1 mg, 62 μmol) was dissolved in 0.5 mL THF-d$_8$ in a J-Young valve NMR tube. [Al(Oct)$_2$H] (80% hydride, 20% [Al(Oct)$_3$], 100.0 μL, 0.257 mmol of hydride) was added followed by the addition of the internal octene mixture (40.0 μL, 0.255 mmol). The solution became light pink over time. The NMR tube was taken out of the glove box and placed in a 40 °C water bath. Within 1 hr, the solution became dark purple. Heating was continued for 48 hr. Analysis by ^{1}H NMR indicated that 74 % of the octene isomers inserted. Continued heating up to 96 hr did not improve the extent of reaction (corresponding to Figure S10).

D$_2$O quench. Following internal olefin insertion attempts, the contents of the NMR tube were placed under vacuum and the un-inserted octenes and solvent removed. The resulting dark purple residue was dissolved in C$_6$D$_6$ and quenched with D$_2$O. The organics were extracted into CDCl$_3$ and analyzed by ^{13}C NMR spectroscopy (Figure S9).

Theoretical Methods

Theoretical calculations throughout this paper were carried out with the Gaussian09[59] program. Geometry optimisations were performed without symmetry constraints using the M06[60-62] functional in combination with the Stuttgart-Dresden[63] (SDD) double-ζ valence basis set and effective core potential (ECP) for Zr and the 6-31G(d) basis set for all other atoms (referred to as BS1). Analytical frequency calculations were carried out to verify structural optimisations and to obtain free energy corrections at the same level of theory (298 K and 1 atm standard state, free energy estimates will differ somewhat in solution and at elevated temperature). All minima contained no imaginary frequencies, and all transition structures contained only one imaginary frequency that exhibited vibrational modes consistent with the anticipated reaction pathway (further verified by optimisation of slightly relaxed transition structures in each direction and IRC calculations). Single point energies for all structures were calculated with the M06 functional with the quadruple-ζ valence def2-QZVP[64,65] basis set and SDD ECP on Zr, and the 6-311+G(2d,p) basis set on all other atoms (referred to as BS2). The Gibbs free energy (ΔG) values reported in this paper were obtained at the M06/BS2//M06/BS1 level.

Monometallic Zr(IV) and Zr(II) complexes were calculated as singlets, as is found experimentally. For bimetallic Zr species, the closed shell singlet, triplet and open shell singlet (antiferromagnetically coupled Zr) were considered. It was found that the triplet and antiferromagnetically coupled singlet complexes had very similar geometries and energies (for complexes **10** and **11** these are included in the Supplementary Information). In Figure 3, all singlet stationary points refer to the closed shell singlet state. Minimum energy crossing points (MECPs) between the two surfaces were located using the methodology of Harvey and co-workers.[57] The barriers for spin state crossing shown in Figure 3 are estimated from electronic energies (E_{elec}) at the M06/BS1 level.

Acknowledgements

Notes and references

‡ The presence of a single broadened Al-CH$_2$ signal at room temperature, which shows splitting at -50 °C (albeit broader still), shows that not only Al-Zr clusters are in equilibrium, but also [Al(Oct)$_3$] which is present in the system is involved in alkyl exchange (see Figure S2).

[1] D. Vogt In *Applied Homogenous Catalysis with Organometallic Compounds*; Cornils, B., Herrmann, W. A., Eds.; VCH: Weinheim, Germany, 1996; Vol. 1, p 245.

[2] P.-A. R. Breuil; L. Magna; H. Olivier-Bourbigou *Catal. Lett.* 2015, **145**, 173.

[3] A. Forestière; H. Olivier-Bourbigou; L. Saussine *Oil & Gas Sci. Technol.* 2009, **64**, 649.

[4] H. Olivier-Bourbigou; A. Forestière; L. Saussine; L. Magna; F. Favre; F. Hugues *Oil Gas Eur. Mag.* 2010, **36**, 97.

[5] G. P. Belov; P. E. Matkovsky *Pet. Chem.* 2010, **50**, 283.

[6] W. Keim *Angew. Chem. Int. Ed.* 2013, **52**, 12492.

[7] J. T. Dixon; M. J. Green; F. M. Hess; D. H. Morgan *J. Organomet. Chem.* 2004, **689**, 3641.

[8] D. S. McGuinness *Chem. Rev.* 2011, **111**, 2321.

[9] T. Agapie *Coord. Chem. Rev.* 2011, **255**, 861.

[10] P. W. N. M. van Leeuwen; N. D. Clément; M. J.-L. Tschan *Coord. Chem. Rev.* 2011, **255**, 1499.

[11] D. F. Wass *Dalton Trans.* 2007, 816.

[12] P. R. Pujado In *Handbook of Petroleum Refining Processes*; 3rd ed.; Meyers, R. A., Ed.; McGraw Hill: 2004, p 5.11.

[13] N. M. Weliange; D. S. McGuinness; J. Patel *Organometallics* 2014, **33**, 4251.

[14] N. M. Weliange; D. S. McGuinness; M. G. Gardiner; J. Patel *Dalton Trans.* 2015, **44**, 15286.

[15] H. C. Brown *Organic syntheses via boranes*; Wiley: New York, 1975.

[16] H. C. Brown; B. C. Subba Rao *J. Org. Chem.* 1957, **22**, 1137.

[17] A. de Klerk; S. W. Hadebe; J. R. Govender; D. Jaganyi; A. B. Mzinyati; R. S. Robinson; N. Xaba *Ind. Eng. Chem. Res.* 2007, **46**, 400.

[18] A. B. Mzinyati; D. Jaganyi *Ind. Eng. Chem. Res.* 2009, **48**, 2770.

[19] U. M. Dzhemilev; A. G. Ibragimov *Russ. Chem. Rev.* 2000, **69**, 121

[20] U. M. Dzhemilev; V. A. D'yakonov *Top. Organomet. Chem.* 2013, **41**, 215.

[21] L. V. Parfenova; L. M. Khalilov; U. M. Dzhemilev *Russ. Chem. Rev.* 2012, **81**, 524.

[22] F. Asinger; B. Fell; R. Janssen; G. Zoche; E. W. Mueller; F. W. A. G. K. Korte *US 3322806 (Shell Oil)* 1967.

[23] E. W. Muller; G. Zoche; F. W. A. G. K. Korte *US 3475477 (Shell Oil)* 1969.

[24] E. J. M. de Boer; H. Van der Heijden; I. Oosterveld; A. Van Zon *WO 2006/005762 (Shell)* 2006.

[25] D. W. Hart; J. Schwartz *J. Am. Chem. Soc.* 1974, **96**, 8115.

[26] J. Schwartz; J. A. Labinger *Angew. Chem. Int. Ed.* 1976, **15**, 333.

[27] L. V. Parfenova; A. V. Balaev; I. M. Gubaidullin; L. R. Abzalilova; S. V. Pechatkina; L. M. Khalilov; S. I. Spivak; U. M. Dzhemilev *Int. J. Chem. Kinet.* 2007, **39**, 333.

[28] L. V. Parfenova; S. V. Pechatkina; L. M. Khalilov; U. M. Dzhemilev *Russ. Chem. Bull. Int. Ed.* 2005, **54**, 316.

[29] L. V. Parfenova; R. F. Vil'danova; S. V. Pechatkina; L. M. Khalilov; U. M. Dzhemilev *J. Organomet. Chem* 2007, **692**, 3424.

[30] E. Y. Pankratyev; T. V. Tyumkina; L. V. Parfenova; L. M. Khalilov; Khursan, S. L.; U. M. Dzhemilev *Organometallics* 2009, **28**, 968.

[31]   E. Y. Pankratyev; T. V. Tyumkina; L. V. Parfenova; S. L. Khursan; L. M. Khalilov; U. M. Dzhemilev *Organometallics* 2011, **30**, 6078.

[32]   L. V. Parfenova; P. V. Kovyazin; I. E. Nifant'ev; L. M. Khalilov; U. M. Dzhemilev *Organometallics* 2015, **34**, 3559.

[33]   L. I. Shoer; K. I. Gell; J. Schwartz *J. Organomet. Chem.* 1977, **136**, C19.

[34]   D. B. Carr; J. Schwartz *J. Am. Chem. Soc.* 1979, **101**, 3521.

[35]   S. M. Baldwin; J. E. Bercaw; H. H. Brintzinger *J. Am. Chem. Soc.* 2008, **130**, 17423.

[36]   S. M. Baldwin; J. E. Bercaw; H. H. Brintzinger *J. Am. Chem. Soc.* 2010, **132**, 13969.

[37]   T. N. Lenton; J. E. Bercaw; V. N. Panchenko; V. A. Zakharov; D. E. Babushkin; I. E. Soshnikov; E. P. Talsi; H. H. Brintzinger *J. Am. Chem. Soc.* 2013, **135**, 10710.

[38]   E.-i. Negishi; T. Yoshida *Tetrahedron Lett.* 1980, **21**, 1501.

[39]   D. E. Van Horn; E.-i. Negishi *J. Am. Chem. Soc.* 1978, **100**, 2252.

[40]   S. Beck; H. H. Brintzinger *Inorg. Chim. Acta* 1998, **270**, 376.

[41]   P. C. Wailes; H. Weigold; A. P. Bell *J. Organomet. Chem* 1972, **43**, C29.

[42]   R. A. Petros; J. R. Norton *Organometallics* 2004, **23**, 5105.

[43]   J. M. Camara; R. A. Petros; J. R. Norton *J. Am. Chem. Soc.* 2011, **133**, 5263.

[44]   M. Bochmann; S. J. Lancaster *Angew. Chem. Int. Ed.* 1994, **33**, 1634.

[45]   M. Bochmann; S. J. Lancaster *J. Organomet. Chem* 1995, **497**, 55.

[46]   E.-i. Negishi; S. J. Holmes; J. M. Tour; J. A. Miller; F. E. Cederbaum; D. R. Swanson; T. Takahashi *J. Am. Chem. Soc.* 1989, **111**, 3336.

[47]   E.-i. Negishi; F. E. Cederbaum; T. Takahashi *Tetrahedron. Lett.* 1986, **27**, 2829.

[48]   T. Cuenca; P. Royo *J. Organomet. Chem.* 1985, **295**, 159.

[49]   S. L. Buchwald; B. T. Watson; J. C. Huffman *J. Am. Chem. Soc.* 1987, **109**, 2544.

[50]   S. Beck; H. H. Brintzinger *Inorg. Chim. Acta* 1998, **270**, 376.

[51]   K. I. Gell; J. Schwartz *J. Chem. Soc. Chem. Comm.* 1979, 244.

[52]   D. R. McAlister; D. K. Erwin; J. E. Bercaw *J. Am. Chem. Soc.* 1978, **100**, 5966.

[53]   P. C. Wailes, Coutts, R. S. P., Weigold, H. *Organometallic Chemistry of Titanium, Zirconium and Hafnium*; Academic Press: New York and London, 1974.

[54]   T. Gibson; L. Tulich *J. Org. Chem.* 1981, **46**, 1821.

[55]   K. I. Gell; B. Posin; J. Schwartz; G. M. Williams *J. Am. Chem. Soc.* 1982, **104**, 1846.

[56]   K. I. Gell; T. V. Harris; J. Schwartz *Inorg. Chem.* 1981, **20**, 481.

[57]   J. N. Harvey; M. Aschi; H. Schwarz; W. Koch *Theor. Chem. Acc.* 1998, **99**, 95.

[58]   E.-i. Negishi; D. Y. Kondakov; D. Choueiry; K. Kasai; T. Takahashi *J. Am. Chem. Soc.* 1996, **118**, 9577.

[59]   M. J. Frisch; G. W. Trucks; H. B. Schlegel; G. E. Scuseria; M. A. Robb; J. R. Cheeseman; G. Scalmani; V. Barone; B. Mennucci; G. A. Petersson; H. Nakatsuji; M. Caricato; X. Li; H. P. Hratchian; A. F. Izmaylov; J. Bloino; G. Zheng; J. L. Sonnenberg; M. Hada; M. Ehara; K. Toyota; R. Fukuda; J. Hasegawa; M. Ishida; T. Nakajima; Y. Honda; O. Kitao; H. Nakai; T. Vreven; J. A. Montgomery Jr.; J. E. Peralta; F. Ogliaro; M. Bearpark; J. J. Heyd; E. Brothers; K. N. Kudin; V. N. Staroverov; R. Kobayashi; J. Normand; K. Raghavachari; A. Rendell; J. C. Burant; S. S. Iyengar; J. Tomasi; M. Cossi; N. Rega; J. M. Millam; M. Klene; J. E. Knox; J. B. Cross; V. Bakken; C. Adamo; J. Jaramillo; R. Gomperts; R. E. Stratmann; O. Yazyev; A. J. Austin; R. Cammi; C. Pomelli; J. W. Ochterski; R. L. Martin; K. Morokuma; V. G. Zakrzewski; G. A. Voth; P. Salvador; J. J. Dannenberg; S. Dapprich; A. D. Daniels; Ö. Farkas; J. B. Foresman; J. V. Ortiz; J. Cioslowski; D. J. Fox *Gaussian 09, Revision D01, Gaussian, Inc., Wallingford CT* 2009.

[60]   Y. Zhao; N. E. Schultz; D. G. Truhlar *J. Chem. Theory Comput.* 2006, **2**, 364.

[61]   Y. Zhao; D. G. Truhlar *J. Chem. Phys.* 2006, **125**, 194101.

[62]   Y. Zhao; D. G. Truhlar *J. Phys. Chem. A* 2006, **110**, 13126.

[63]   D. Andrae; U. Häussermann; M. Dolg; H. Stoll; H. Preuss *Theoret. Chim. Acta* 1990, **77**, 123.

[64]   F. Weigend; R. Ahlrichs *Phys. Chem. Chem. Phys.* 2005, **7**, 3297.

[65]   F. Weigend; F. Furche; R. Ahlrichs *J. Chem. Phys.* 2003, **119**, 12753.

Table of Contents Entry:

The insertion of internal olefins and chain walking isomerisation at di-*n*-octylaluminium hydride [Al(Oct)$_2$H], promoted by zirconocene dichloride [Cp$_2$ZrCl$_2$] has been studied.